Molecular Crystals and Liquid Crystals

Publication details, including instructions for authors and subscription information:
http://www.tandfonline.com/loi/gmcl20

INTERACTION BETWEEN SPHERICAL PARTICLES IN A DEFORMED LIQUID CRYSTAL

Jun-ichi Fukuda [a], Keiko M. Aoki [a], Bohdan I. Lev [a b] & Hiroshi Yokoyama [a c]

[a] Yokoyama Nano-structured Liquid Crystal Project, ERATO, Japan Science and Technology Agency, 5-9-9 Tokodai, Tsukuba 300-2635, Japan

[b] Department of the theoretical physics, Institute of Physics, NAS Ukraine, Prospekt Nauki 46, Kyiv 04022, Ukraine

[c] Nanotechnology Research Institute, AIST, 1-1-4 Umezono, Tsukuba 305-8568, Japan

Version of record first published: 07 Jan 2010

To cite this article: Jun-ichi Fukuda, Keiko M. Aoki, Bohdan I. Lev & Hiroshi Yokoyama (2004): INTERACTION BETWEEN SPHERICAL PARTICLES IN A DEFORMED LIQUID CRYSTAL, Molecular Crystals and Liquid Crystals, 413:1, 211-220

To link to this article: http://dx.doi.org/10.1080/15421400490437132

Mol. Cryst. Liq. Cryst., Vol. 413, pp. 211/[2347]–220/[2356], 2004

ISSN: 1542-1406 print/1563-5287 online
DOI: 10.1080/15421400490437132

Taylor & Francis
Taylor & Francis Group

INTERACTION BETWEEN SPHERICAL PARTICLES IN A DEFORMED LIQUID CRYSTAL

Jun-ichi Fukuda and Keiko M. Aoki
Yokoyama Nano-structured Liquid Crystal Project, ERATO, Japan Science and Technology Agency, 5-9-9 Tokodai, Tsukuba 300-2635, Japan

Bohdan I. Lev
Yokoyama Nano-structured Liquid Crystal Project, ERATO, Japan Science and Technology Agency, 5-9-9 Tokodai, Tsukuba 300-2635, Japan
and
Department of the theoretical physics, Institute of Physics, NAS Ukraine, Prospekt Nauki 46, Kyiv 04022, Ukraine

Hiroshi Yokoyama
Yokoyama Nano-structured Liquid Crystal Project, ERATO, Japan Science and Technology Agency, 5-9-9 Tokodai, Tsukuba 300-2635, Japan
and
Nanotechnology Research Institute, AIST, 1-1-4 Umezono, Tsukuba 305-8568, Japan

We study how the initial deformation of a nematic liquid crystal affects the interaction between particles mediated by the elastic deformation of a nematic liquid crystal. We calculate the interaction energy between particles in a hybrid nematic cell, homeotropic on the surface of one confining plate and tangential (director can rotate freely) on the other. We find an analytic form of the interaction energy in the case of weak anchoring on the surface of the particle. This interaction energy can be non-monotonic and have a minimum in its landscape, which makes a clear contrast to that in a uniform nematic liquid crystal.

Keywords: colloid; elastic deformation; hybrid nematic cell; interaction; nematic liquid crystal

Address correspondence to Jun-ichi Fukuda, Yokoyama Nano-Structured Liquid Crystal Project, ERATO, Japan Science and Technology Agency, 5-9-9 Tokodai, Tsukuba, 300-2635, Japan.

INTRODUCTION

Much attention has been paid to colloidal systems and emulsions in fundamental science as well as in technology. Of much interest is how constituent particles or droplets in such systems interact with each other and what kind of structures and phases will be observed by controlling these interactions.

Recently, colloidal suspensions and emulsions with anisotropic host fluids like liquid crystals have attracted a great deal of interest as a new class of composite materials [1–3]. One of the interesting and important properties of liquid crystal emulsions and colloids is that the particles can interact via the elastic deformation of liquid crystals arising from the surface anchoring of the particles. This novel elasticity-mediated interaction has proven to play a crucial role in yielding a wide variety of superstructures that have not been observed in conventional colloidal systems. Striking examples of such superstructures experimentally observed include a linear-chain superstructure [2,4–6] and anisotropic clusters [1,7]. Periodic lattices originating purely from this interaction have also been reported [8]. The understanding of the elasticity-mediated interaction is therefore quite important to predict essential properties and behaviors of superstructures in liquid crystal colloids and emulsions.

There have been several theoretical attempts to evaluate this elasticity-mediated interaction [9,10] and recently, one of the present authors (B.I.L.) has developed a theoretical scheme of calculating the interaction potential [11]. This scheme has proved to be quite useful because it can be applied to general cases without assuming high symmetry of the particles. Moreover, it can be extended to a case of a non-uniform liquid crystal like a cholesteric [12]. In our previous study [13] we calculated the particle interaction energy in a hybrid nematic cell, where one boundary imposes strong homeotropic anchoring and on the other boundary the nematic orientation is fixed along a direction parallel to the boundary. It was motivated by a recent experiment [8] showing the formation of a two-dimensional crystal structure by glycerol droplets dispersed in a nematic liquid crystal. In this experiment, the liquid crystal faces with the air at the upper boundary, which leads to the homeotropic orientation there. On the other hand, liquid crystal molecules tend to align parallel to the lower boundary. Our previous calculations showed that the interaction energy landscape is far more complex than that in a uniform nematic, which might lead to rich and non-trivial structure formation. However, our theoretical setup was different from that in the experiment [8] in that liquid crystal orientation on the lower boundary is fixed in our calculation. In this article we will present the calculation of elasticity-mediated

interaction energy in a setup similar to the experiment, that is, strong homeotropic anchoring is imposed on one boundary and on the other boundary tangential anchoring without any preference for inplane orientation is assumed.

CALCULATION OF THE INTERACTION POTENTIAL

Formulation of the Problem

We consider a nematic liquid crystal confined between two parallel plates with the distance d as depicted in Figure 1. We set the z-axis perpendicular to the plates and we set the origin so that the two plates are located at $z = 0$ and d. We impose strong homeotropic alignment at $z = d$ and tangential boundary condition at $z = 0$ without any preference for the in-plane orientation. This geometrical setup is similar to that in the experiment by Nazarenko *et al.* [8]. For simplicity we assume one-constant approximation in the Frank elastic energy. When we take the x-axis parallel to the direction of nematic orientation at $z = 0$, it is easy to show that the ground state of the director field is

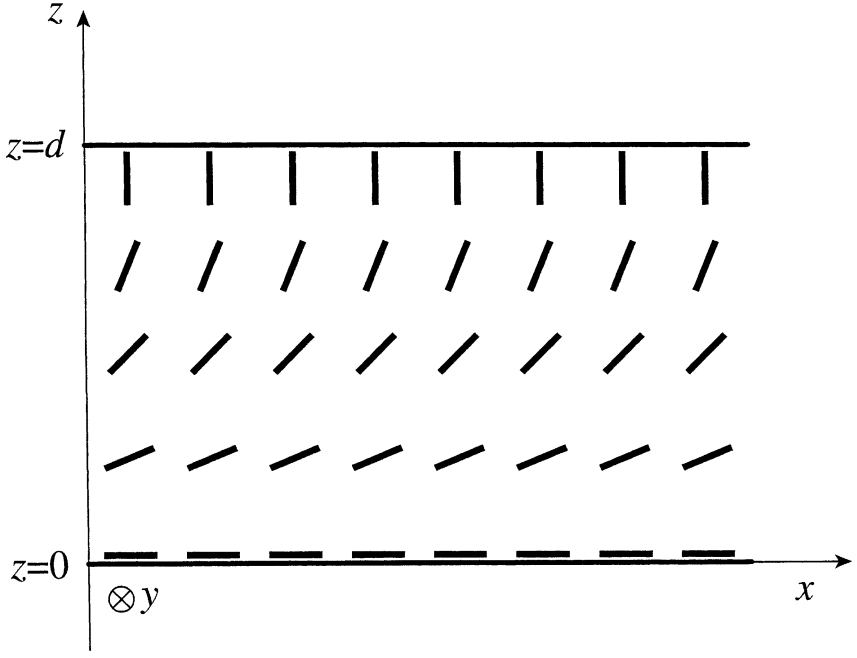

FIGURE 1 Illustration of the geometry of our system.

$$\boldsymbol{n}^{(0)}(z) = (\cos q_0 z, 0, \sin q_0 z), \tag{1}$$

with $q_0 \equiv \pi/2d$. To describe the deformation of the director field with respect to the ground state, we introduce the deformation fields $u(\boldsymbol{r})$ and $v(\boldsymbol{r})$ and the director field $\boldsymbol{n}(\boldsymbol{r})$ can be written as

$$\boldsymbol{n}(\boldsymbol{r}) = (\cos(q_0 z + u(\boldsymbol{r}))\cos v(\boldsymbol{r}), \sin v(\boldsymbol{r}), \sin(q_0 z + u(\boldsymbol{r}))\cos v(\boldsymbol{r})). \tag{2}$$

The bulk Frank elastic energy in the one-constant approximation can be written as [14]

$$F_b = \frac{1}{2}K \int d^2\boldsymbol{r}_\perp \int_0^d dz\{(\nabla \cdot \boldsymbol{n})^2 + (\nabla \times \boldsymbol{n})^2\}, \tag{3}$$

with K being the elastic constant and $\boldsymbol{r}_\perp = (x, y)$. We substitute Eq. (2) into Eq. (3) to describe the elastic energy in terms of the deformation fields u and v. Throughout this argument we restrict ourselves to the case of small deformations and we retain up to second order terms in u and v as in our previous study [11,12]. After some calculations, we arrive at

$$F_b = \frac{1}{2}K \int d^2\boldsymbol{r}_\perp \int_0^d dz\{(\nabla u)^2 + (\nabla v)^2 - q_0^2 v^2\}. \tag{4}$$

Here we introduce the Fourier transform, taking the boundary conditions at $z = 0$ and d into account ($u = v = 0$ at $z = d$ and $u = \partial v/\partial z = 0$ at $z = 0$), as

$$u(\boldsymbol{q}_\perp, 2mq_0) = \int d^2\boldsymbol{r}_\perp \int_0^d dz e^{-iq_\perp \cdot \boldsymbol{r}_\perp} \sin 2mq_0 z\, u(\boldsymbol{r}), \tag{5}$$

$$v(\boldsymbol{q}_\perp, (2m-1)q_0) = \int d^2\boldsymbol{r}_\perp \int_0^d dz e^{-iq_\perp \cdot \boldsymbol{r}_\perp} \sin(2m-1)q_0 z\, v(\boldsymbol{r}), \tag{6}$$

with m being a positive integer. Then from Eq. (4), (5) and (6), we have

$$\begin{aligned} F_b = \frac{1}{2}K \frac{1}{(2\pi)^2} \int d^2\boldsymbol{q}_\perp \cdot \frac{2}{d} \sum_{m=1}^{\infty} \\ \times \Big\{ (\boldsymbol{q}_\perp^2 + (2mq_0)^2) u(\boldsymbol{q}_\perp, 2mq_0) u(-\boldsymbol{q}_\perp, 2mq_0) \\ + (\boldsymbol{q}_\perp^2 + ((2m-1)^2 - 1)q_0^2) \\ \times v(\boldsymbol{q}_\perp, (2m-1)q_0) v(-\boldsymbol{q}_\perp, (2m-1)q_0) \Big\}. \end{aligned} \tag{7}$$

Next we consider how particles introduced in our system deform the director field. We write the surface energy on the particles in the Rapini-Papoular form [15] as $F_s = \sum_p \oint_{\Omega_p} d^2S W(\boldsymbol{s})(v(\boldsymbol{s}) \cdot \boldsymbol{n}(\boldsymbol{s}))^2$. Here p is the index labeling the particles and the surface of the particle p is denoted by $\boldsymbol{\Omega}_p$. The integral is taken over $\boldsymbol{\Omega}_p$ and d^2S is the surface element. The anchoring strength is given by $W(\boldsymbol{s})$ and $v(\boldsymbol{s})$ is the unit normal to the surface at the point $\boldsymbol{s}$. In the case of homeotropic anchoring, $W(\boldsymbol{s}) < 0$ and vice versa for planar anchoring. We restrict ourselves to the case of weak anchoring ($|W|r_0/K \ll 1$, where r_0 is the characteristic dimension of the particles) so that the director field is only slightly deformed by the particles from its ground state (Eq. (1)).

In dealing with the surface energy, we make a gradient expansion of the director field $\boldsymbol{n}(\boldsymbol{s})$ around the center of gravity of the particle p, which we will denote by $\boldsymbol{r}^{(p)}$. We can formally write the director field as $\boldsymbol{n} = \boldsymbol{n}^{(0)} + \delta\boldsymbol{n}$, with $\boldsymbol{n}^{(0)}$ being the initial director field in the absence of particles defined in Eq. (1). After some calculations, we find $(v(\boldsymbol{s}) \cdot \boldsymbol{n}(\boldsymbol{s}))^2 \simeq \mathcal{A}^{(p)}_{kl}((1/2)n^{(0)}_k(\boldsymbol{r}^{(p)}) n^{(0)}_l(\boldsymbol{r}^{(p)}) + n^{(0)}_k(\boldsymbol{r}^{(p)})\delta n_l(\boldsymbol{r}^{(p)}))$, for the pth particle. Here we have defined the operator $\mathcal{A}^{(p)}_{kl} = \alpha^{(p)}_{kl} + \beta^{(p)}_{jkl}\partial^{(p)}_j + \gamma^{(p)}_{ijkl}\partial^{(p)}_i\partial^{(p)}_j$ with $\partial^{(p)}_j \equiv \partial/\partial r^{(p)}_j$, and $\alpha^{(p)}_{kl}, \beta^{(p)}_{jkl}$ and $\gamma^{(p)}_{ijkl}$ are the tensors characterizing the geometry of the particles defined in [11]. Noticing that $\delta\boldsymbol{n}(\boldsymbol{r}^{(p)}) \simeq (-u(\boldsymbol{r}^{(P)}) \sin q_0 r^{(p)}_z,\ v(\boldsymbol{r}^{(p)}),\ u(\boldsymbol{r}^{(p)}) \cos q_0 r^{(p)}_z)$ (from Eq. (2)) and using Eq. (1), we obtain the resultant form of the surface energy as

$$
\begin{aligned}
F_s =& \frac{1}{2}\sum_p \mathcal{A}^{(p)}_{kl}\left(n^{(0)}_k\left(\boldsymbol{r}^{(p)}\right) n^{(0)}_l\left(\boldsymbol{r}^{(p)}\right)\right) \\
&+ \sum_p \left\{ \frac{1}{2}\left(\mathcal{A}^{(p)}_{zz} - \mathcal{A}^{(p)}_{xx}\right)\left(u\left(\boldsymbol{r}^{(p)}\right) \sin 2q_0 r^{(p)}_z\right)\right. \\
&\quad + \mathcal{A}^{(p)}_{xz}\left(u\left(\boldsymbol{r}^{(p)}\right) \cos 2q_0 r^{(p)}_z\right) \\
&\quad \left. + \mathcal{A}^{(p)}_{xy}\left(v\left(\boldsymbol{r}^{(p)}\right) \cos q_0 r^{(p)}_z\right) + \mathcal{A}^{(p)}_{yz}\left(v\left(\boldsymbol{r}^{(p)}\right) \sin q_0 r^{(p)}_z\right)\right\}. \quad (8)
\end{aligned}
$$

In this article we discuss only the case of spherical particles. Then we find from Ref. [11] that

$$
\frac{1}{2}\left(\mathcal{A}^{(p)}_{zz} - \mathcal{A}^{(p)}_{xx}\right) = \Gamma\left((\partial^{(p)}_z)^2 - (\partial^{(p)}_x)^2\right),\ \mathcal{A}^{(p)}_{ij} = 2\Gamma\partial^{(p)}_i\partial^{(p)}_j\ (i \neq j), \quad (9)
$$

where $\Gamma \equiv 4\pi W r_0^4/15$ with r_0 being the radius of the particle.

Interaction Energy

Now we proceed to the calculation of the elasticity-mediated interaction energy. The total energy of the system is the sum of the bulk energy F_b (Eq. (4)) and the surface energy F_s (Eq. (8)). The orientation profile that minimizes the total energy $(u_{\min}, v_{\min})$ is determined by the conditions $\delta(F_b+F_s)/\delta u(\boldsymbol{q}_\perp, 2mq_0)|_{u_{\min},v_{\min}} = \delta(F_b+F_s)/\delta v(\boldsymbol{q}_\perp,(2m-1)q_0)|_{u_{\min},v_{\min}} = 0$. Substituting the profile $(u_{\min}, v_{\min})$ and picking up the terms taking care of the interaction between the particles as in [11,13], we can write the interaction energy $U_{pp'}$ as

$$\begin{aligned} U_{pp'}(\boldsymbol{r}^{(p)}, \boldsymbol{r}^{(p')}) = -\frac{1}{K}\frac{1}{(2\pi)^2}\int d^2\boldsymbol{q}_\perp \cdot \frac{2}{d}\sum_{m=1}^{\infty} \\ \times \left[\frac{1}{\boldsymbol{q}_\perp^2 + (2mq_0)^2} \mathcal{D}_1^{(p)} \mathcal{D}_1^{(p')} e^{-i\boldsymbol{q}_\perp \cdot \boldsymbol{r}_\perp^{(pp')}} \right. \\ \times \sin 2mq_0 r_z^{(p)} \sin 2mq_0 r_z^{(p')} \\ + \frac{1}{\boldsymbol{q}_\perp^2 + ((2m-1)^2 - 1)q_0^2} \mathcal{D}_2^{(p)} \mathcal{D}_2^{(p')} e^{-i\boldsymbol{q}_\perp \cdot \boldsymbol{r}_\perp^{(pp')}} \\ \left. \times \cos(2m-1)q_0 r_z^{(p)} \cos(2m-1)q_0 r_z^{(p')} \right]. \end{aligned} \tag{10}$$

where $\boldsymbol{r}_\perp^{(pp')} \equiv \boldsymbol{r}_\perp^{(p)} - \boldsymbol{r}_\perp^{(p')}$ and we have defined the operators

$$\begin{aligned} \mathcal{D}_1^{(p)} g\left(\boldsymbol{r}^{(p)}\right) = \frac{1}{2}\left(\mathcal{A}_{zz}^{(p)} - \mathcal{A}_{xx}^{(p)}\right)\left(g\left(\boldsymbol{r}^{(p)}\right) \sin 2q_0 r_z^{(p)}\right) \\ + \mathcal{A}_{xz}^{(p)}\left(g\left(\boldsymbol{r}^{(p)}\right) \cos 2q_0 r_z^{(p)}\right), \end{aligned} \tag{11}$$

$$\mathcal{D}_2^{(p)} g\left(\boldsymbol{r}^{(p)}\right) = \mathcal{A}_{xy}^{(p)}\left(g\left(\boldsymbol{r}^{(p)}\right) \cos q_0 r_z^{(p)}\right) + \mathcal{A}_{yz}^{(p)}\left(g\left(\boldsymbol{r}^{(p)}\right) \sin q_0 r_z^{(p)}\right), \tag{12}$$

with g being an arbitary function. After some calculations similar to those in [13], we obtain

$$\begin{aligned} U_{pp'}\left(\boldsymbol{r}^{(p)}, \boldsymbol{r}^{(p')}\right) = -\frac{1}{4\pi K}\left[\mathcal{D}_1^{(p)}\mathcal{D}_1^{(p')}\left(h_1\left(|\boldsymbol{r}_\perp^{(pp')}|, r_z^{(p)} - r_z^{(p')}\right)\right.\right. \\ - h_1\left(|\boldsymbol{r}_\perp^{(pp')}|, r_z^{(p)} + r_z^{(p')}\right)\Big) \\ + \mathcal{D}_2^{(p)}\mathcal{D}_2^{(p')}\left(h_2\left(|\boldsymbol{r}_\perp^{(pp')}|, r_z^{(p)} - r_z^{(p')}\right)\right. \\ \left.\left. + h_2\left(|\boldsymbol{r}_\perp^{(pp')}|, r_z^{(p)} + r_z^{(p')}\right)\right)\right], \end{aligned} \tag{13}$$

where $\boldsymbol{r}_\perp^{(pp')} = \boldsymbol{r}_\perp^{(p)} - \boldsymbol{r}_\perp^{(p^\perp)}$ and

$$h_1(\xi,\eta)=\frac{1}{\sqrt{\xi^2+\eta^2}}+\sum_{m=1}^{\infty}\left\{\frac{1}{\sqrt{\xi^2+(\eta-2md)^2}}+\frac{1}{\sqrt{\xi^2+(\eta+2md)^2}}-\frac{1}{md}\right\}, \tag{14}$$

$$h_2(\xi,\eta)=\frac{\cos\left(q_0\sqrt{\xi^2+\eta^2}\right)}{\sqrt{\xi^2+\eta^2}}+\sum_{m=1}^{\infty}\left[(-1)^m\left\{\frac{\cos\left(q_0\sqrt{\xi^2+(\eta-2md)^2}\right)}{\sqrt{\xi^2+(\eta-2md)^2}}+\frac{\cos\left(q_0\sqrt{\xi^2+(\eta+2md)^2}\right)}{\sqrt{\xi^2+(\eta+2md)^2}}\right\}-\frac{1}{md}\right]. \tag{15}$$

We note that $h_2(\xi,\eta)$ is associated with the variable v and its oscillating nature may be attributed to the presence of negative contribution $-q_0^2v^2$ in the free energy (4). This negative contribution reflects the fact that the initial deformed state is not a ground state and stabilized by the imposed boundary conditions.

DISCUSSION

Since the resultant form the interaction energy (13) is still complicated, we present the form of the interaction energy obtained numerically for one specific case where $r_z^{(p)}=r_z^{(p')}$ and the particles are close to the upper confining plate imposing homeotropic anchoring. This situation closely resembles that in the experiments of Ref. [8]. We note that the numerical results presented below have been obtained with the aid of Maple™ 6.01.

In Figure 2 we plot the reduced interaction energy $\bar{U}_{pp'}\equiv 4\pi Kd^5U_{pp'}/\Gamma^2$ as a function of the inter-particle distance r in the case of $r_z^{(p)}=r_z^{(p')}=0.9d$ and $0.8d$. We let ϕ denote the angle between the x-axis and $\boldsymbol{r}_\perp^{(pp')}$ and the curves in Figure 2 are plotted for fixed ϕ's as functions of reduced inter-particle distance $r/d=|\boldsymbol{r}_\perp^{(pp')}|/d$. We find from Figure 2 that $\overline{U}_{pp'}$ has its minimum for ϕ smaller than some threshold value ($\simeq 45^\circ$) and purely repulsive otherwise. For $r\to 0$, the interaction is repulsive for all cases. When the interaction potential has its minimum, the minimum position r becomes smaller and the absolute value of the minimum energy becomes larger for smaller ϕ and $r_z^{(p)}$. These energy landscape indicate that two particles tend to align parallel to the x-axis (the direction of the planar orientation on the lower boundary) while keeping some finite distance. We also note that

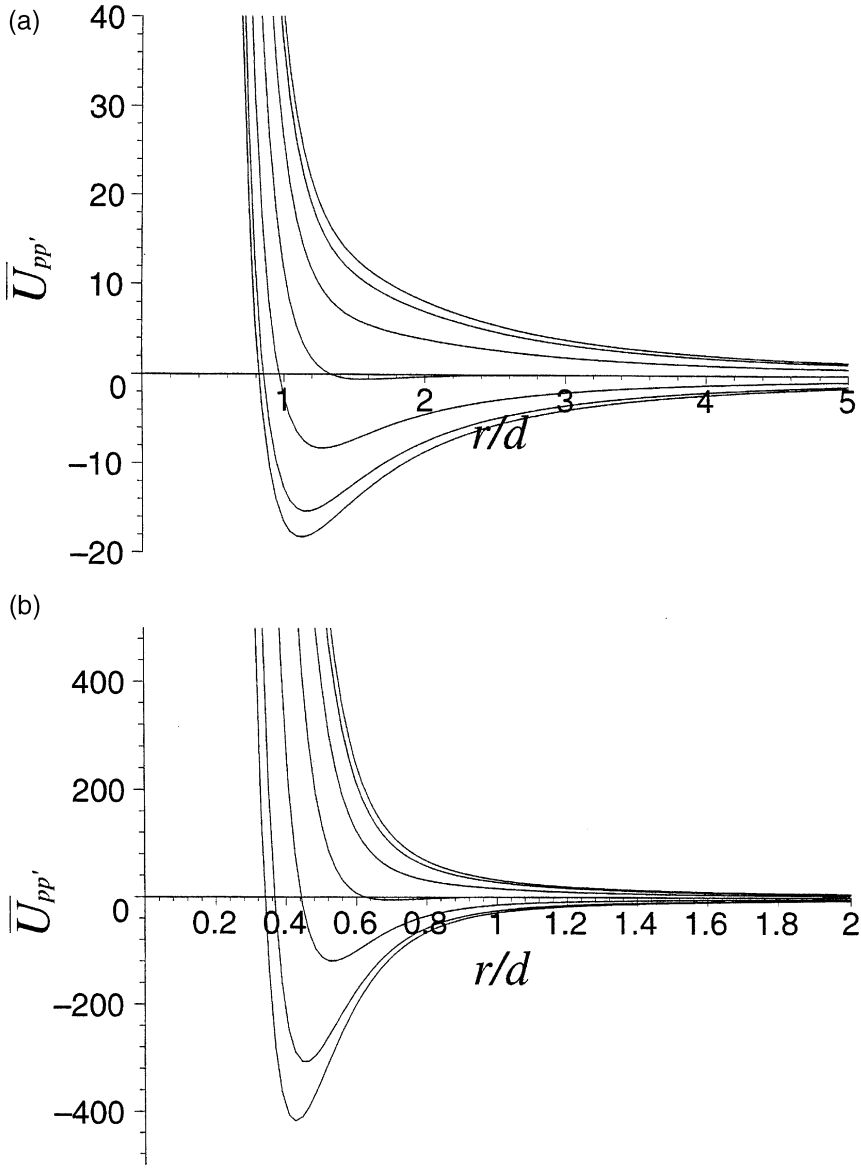

FIGURE 2 Reduced pairwise interaction energy $\overline{U}_{pp'} \equiv 4\pi K d^5 U_{pp'}/\Gamma^2$ as a function of reduced particle distance $r/d = |\boldsymbol{r}_\perp^{pp'}|/d$ for (a) $r_z^{(p)} = r_z^{(p')} = 0.9d$ and (b) $r_z^{(p)} = r_z^{(p')} = 0.8d$. The curves correspond to $\phi = 0°$, $15°$, $30°$, $45°$, $60°$ and $90°$ from bottom to top, where ϕ is the angle between $\boldsymbol{r}_\perp^{(pp')}$ and the x-axis.

these results are qualitatively similar to those in our previous study [13], where we dealt with a case of fixed director orientation on one confining plate with planar anchoring. However, for $r_z^{(p)} = 0.9$ quantitative difference in striking because in the latter case the minimum value of $\bar{U}_{pp'}$ is approximately ~ -0.5 and the interaction is purely repulsive for ϕ that is as small as 30° [13].

CONCLUSION

In this article we have calculated the liquid-crystal-mediated interaction energy between spherical particles immersed in a hybrid nematic cell. The boundary conditions of the hybrid nematic cell are strong homeotropic anchoring on the surface of one confining plate and tangential anchoring without any preference for the in-plane orientation on the other. We have given an analytic form of the interaction energy in the case of weak anchoring on the surface of the particles. The resultant form of the interaction energy is much more complex than that in the case of a uniform nematic, which reflects the presence of the initial deformed structure of nematic liquid crystal due to the boundary conditions.

By evaluating the interaction energy numerically, we have presented the energy landscape in a case similar to a recent experiment by Nazarenko *et al*. where two particles are close to one confining plate imposing strong homeotropic anchoring. From this energy landscape we propose a possibility of forming a new type of chain-like structures whose inter-particle distance depends on the distance between a particle and a confining surface as well as that between two confining surfaces. Strong quantitative difference are found from our previous study where in plane orientation was fixed on the surface with planar anchoring. In a future article we will give a detailed argument on the interaction energy landscape in different cases and the difference arising form the boundary condition.

REFERENCES

[1] Poulin, P., Raghunathan, V. A., Richetti, P., & Roux, D. (1994). *J. Phys. II (France)*, *4*, 1557.
[2] Poulin, P., Stark, H., Lubensky, T. C., & Weitz, D. A. (1997). *Science*, *275*, 1770.
[3] Meeker, S. P., Poon, W. C. K., Crain, J., & Terentjev, E. M. (2000). *Phys. Rev. E*, *61*, R6083.
[4] Poulin, P. & Weitz D. A. (1998). *Phys. Rev. E*, *57*, 626.
[5] Loudet, J.-C., Barois, P., & Poulin, P. (2000). *Nature (London)*, *407*, 611.
[6] Poulin, P., Francès, N., & Mondain-Monval, O. (1999). *Phys. Rev. E*, *59*, 4384.
[7] Mondain-Monval, O., Dedieu, J. C., Gulik-Krzywicki, T., & Poulin, P. (1999). *Eur. Phys. J. B.*, *12*, 167.

[8] Nazarenko, V. G., Nych, A. B., & Lev, B. I. (2001). *Phys. Rev. Lett.*, *87*, 075504.
[9] Ramaswamy, S., Nityananda, R., Raghunathan, V. A., & Prost, J. (1996). *Mol. Cryst. Liq. Cryst.*, *288*, 175.
[10] Ruhwandl, R. W. & Terentjev, E. M. (1997). *Phys. Rev. E*, *55*, 2958.
[11] Lev, B. I. & Tomchuk, P. M. (1999). *Phys. Rev. E*, *59*, 591.
[12] Fukuda, J., Lev, B. I., & Yokoyama, H. (2002). *Phys. Rev. E*, *65*, 031710.
[13] Fukuda, J., Lev, B. I., Aoki, K. M., & Yokoyama, H. (2002). *Phys. Rev. E*, *66*, 051711.
[14] de Gennes, P. G. & Prost, J. (1993). *The physics of liquid crystals*, 2nd edn., Oxford University Press.
[15] Rapini, A. & Papoular, M. (1969). *J. Phys. Colloq.*, *30*, C4–54.